Efficient degradation of metronidazole in wastewater by FeO$_x$/GAC catalytic ozonation

Na Wang[1,2] · Chenxi Zhan[1] · Junzhuo Li[1] · Dan Liu[1] · Junjie Xiong[1] · Geshan Zhang[1] · Yin-an Ming[1]

Abstract

To remove the metronidazole, the iron oxides loaded on granular activated carbon (FeO$_x$-GAC) were prepared by the impregnation–calcination approach. The physicochemical properties of the catalysts were characterized by electron microscopy (SEM), transmission electron microscopy (TEM), Fourier transform infrared spectroscopy (FTIR), X-ray diffraction (XRD) and X-ray photoelectron spectroscopy (XPS). The results show that FeO$_x$-GAC has a porous structure, in which the iron oxides with a variety of valence states are smoothly attached on the activated carbon. The catalytic activity of FeO$_x$-GAC was evaluated for metronidazole removal, exhibiting great catalytic efficiency of the catalyst. Besides, the catalytic ozonation of metronidazole was optimized by varying the dose of ozone and catalyst, as well as the pH of the solution.

Introduction

Due to the rapid development of industry in China, the discharge of industrial wastewater is increasing, whose composition is extremely complex. Many organic pollutants, e.g., heterocyclic compounds, are difficult to remove through normal biological techniques. Nitroimidazoles, such as metronidazole, are antibiotics widely used for the treatment of bacterial infection, which is difficult to degrade due to the complex structure. Ineffective treatment of pharmaceutical, wastewater would result in critical problems of environment [1]. Bergeron et al. [2] analyzed a rural drinking water in the United States and found drug-resistant genes and drug-resistant bacteria in the raw water. Besides, study has shown that nitroimidazoles have serious potential harmful effects

such as cell mutagenesis and animal carcinogenesis [3]. Metronidazole is widely applied for anaerobic infections of humans and animals, which can control various protozoal diseases due to its strong anti-anaerobic and anti-protozoal activity as well as its low price [4]. However, water-soluble metronidazole is non-biodegradable and easy to accumulate [5]. Residual metronidazole is often found in the effluent of pharmaceutical wastewater treatment plants and medical wastewater, which threaten the safety of human health and environment [6]. Therefore, it is important to effectively remove metronidazole in water.

Ozonation is receiving great attention in wastewater treatment because of its good oxidation capacity, absent secondary pollution, and its ability to improve the biochemical properties of wastewater. However, ozonation alone suffers the problem of low ozone utilization rate, insufficient oxidation capacity, and certain selectivity for organic pollutants, making the treatment unsatisfactory [7–9]. Catalytic ozonation is the oxidation technique of organic pollutants in water by active oxidizing species (e.g., OH radical) with greater oxidizing ability, which can be produced by catalyst-initiated ozone decomposition. This technique is of high reaction efficiency without oxidizing selectivity, and hence can decompose organic pollutants more thoroughly [10–13]. Catalytic ozonation includes homogeneous catalytic ozonation and heterogeneous catalytic ozonation. Regarding homogeneous catalytic ozonation, metal ions, such as Fe^{2+}, Mn^{2+}, Cu^{2+}, Co^{2+}, Ag^+, Ni^{2+}, Zn^{2+}, etc., are common catalysts [14, 15]. Although they can react adequately with ozone and

Na Wang and Chenxi Zhan contributed equally to this work and should be considered co-first authors.

Geshan Zhang and Yin-an Ming are contributed equally to this work.

✉ Geshan Zhang
75320932@qq.com

✉ Yin-an Ming
mingyinan@wit.edu.cn

1 School of Chemical and Environmental Engineering, Wuhan Institute of Technology, Wuhan 430205, Hubei, China

2 Zhongnai Technology (Wuhan) Co., Ltd., Wuhan 430080, Hubei, China

organic pollutants with high catalytic efficiency, their loss in treated water after treatment as well as their secondary pollution are fatal drawbacks that limit their applications. These problems can be solved by heterogeneous catalysts, which usually are metal oxides with abundant active catalytic sites on their surface [16–18]. However, there is still problem of insufficient reaction efficiency of active component with ozone and organic pollutants due to the spatial site resistance caused by catalyst support. Therefore, the selection of active components and corresponding supports is crucial for the preparation of catalysts. Transition metals are often applied as catalysts in heterogeneous catalytic ozonation. Chen et al. prepared ZSM5 zeolites loaded with cerium, iron, or manganese oxides for catalytic ozonation of nitrobenzene in water [19]. Yan et al. synthesized $ZnFe_2O_4$/ZnNCN nanocomposites via hydrothermal and high temperature calcination methods and applied in heterogeneous catalytic ozonation [20]. Among them, iron oxides have been reported to be effective for catalytic ozonation [10–12] and can be produced in large quantities through industrial practice due to their low cost and abundant reserves. Besides, the research regarding iron oxides-based catalyst applied in catalytic ozonation for nitroimidazoles (i.e., metronidazole) removal has not been reported, which deserves scientific investigation to provide fundamental support for practical application.

In this study, the iron oxides were selected as active component and granular activated carbon is selected as catalyst support. The granular activated carbon (GAC) has large specific surface area and well-developed pore structure which can provide a large number of active sites for catalytic reactions and improve the adsorption of organic pollutants on the surface, eventually facilitating the catalytic reactions [21–25]. Iron oxides loaded on granular activated carbon can be prepared by impregnation–calcination approach [26], which is modified and applied in this work. The physicochemical properties of the catalysts were characterized using various techniques. The catalytic activity of iron oxides/granular activated carbon (FeO_x-GAC) was evaluated in catalytic ozonation for metronidazole removal, and the effectiveness of FeO_x-GAC on ozone decomposition was also investigated.

Preparation of catalyst

Materials and reagents

The ferric nitrate ninhydrous ($Fe(NO_3)_3 \cdot 9H_2O$), metronidazole, tert-butyl alcohol, sodium hydroxide (NaOH) and hydrochloric acid (HCl) used in the experiment were purchased from Sinopharm Chemical Reagent Group. $Fe(NO_3)_3 \cdot 9H_2O$ was used as the precursor of the iron oxides

catalyst, metronidazole dissolved in distilled water was used as the target contaminant, and tert-butanol was used as a hydroxyl radical scavenger. Hydrochloric acid (HCl) and sodium hydroxide (NaOH) were applied to adjust the pH of metronidazole aqueous solution. Granular activated carbon was purchased from Yicheng Synthetic Mechanical and Electrical Co., Ltd and used as the support for the catalyst. All chemicals are at least analytical grade or higher without further purification unless indicated.

Catalyst preparation methods

After method screening, the catalyst was prepared using impregnation–calcination method. The granular activated carbon was rinsed with distilled water and then dried in oven at 100 ℃. The activated carbon and $Fe(NO_3)_3 \cdot 9H_2O$ in the mass ratio of 10:1 were placed in a conical flask, and distilled water was added until the liquid level over the activated carbon. Then, the conical flask was placed in a thermostatic water bath at 30℃ for 12 h to ensure the active component fully adsorbed on the activated carbon. The treated activated carbon was washed 1–2 times with distilled water and dried in oven at 100 ℃. The catalyst was calcined in a muffle furnace at the rate of 2 ℃/min to 350 ℃ for 3 h and cooled naturally to obtain the catalyst FeO_x-GAC.

Characterization of catalysts

The morphology and elemental composition were analyzed by scanning electron microscopy (SEM, JSM-5510LV) and transmission electron microscopy (TEM, JSM-5510LV). The crystalline pattern was determined by D8 ADV and powder X-ray diffraction (XRD) with copper Kα radiation at a scan rate of 4°/min from 10° to 90°. The X-ray photoelectron spectroscopy (XPS) measurements were performed on an ESCALAB Xi$^+$ spectrometer (Hot Fisher, USA) using monochromated aluminum Kα300 watt radiation.

Experimental methods

Catalytic ozonation and single ozonation were performed in 250 mL porous gas washing bottles. Ozone was produced from pure oxygen by CFG-20Y laboratory ozone generator (Meites, China). The reactor was filled with 200 mL of metronidazole solution with the concentration of 100 mg/L. 0.4 g catalyst was added in the reactor with continuous stirring and the ozone was continuously bubbled into the reactor at different rates of gas flow. The reaction temperature was kept at 25 °C. The excess ozone after the reaction was absorbed by 20% potassium iodide solution. Unless otherwise specified, the initial pH was adjusted to neutral by 0.1 M hydrochloric acid or sodium hydroxide. At certain time interval, the sample was collected and a small amount of $Na_2S_2O_3$

(0.2 M) was added to quench the residual ozone reaction. After filtering through a 0.225 μm filter, the concentration of metronidazole was measured with UV spectrophotometry at the absorbance of 320 nm.

Results and discussion

Characterization of catalysts

The prepared catalyst of FeO$_x$-GAC and GAC were analyzed by SEM to observe its surface morphology, as shown in Fig. 1. It can be seen that GAC has a porous structure (Fig. 1a) and the surface changes significantly after loading iron oxides with many particles (dozens to hundreds of nanometers in size) attached on its surface (Fig. 1b). To further understand the amount of loading and the surface element distribution, the EDS analysis was performed, and the results are shown in Fig. 1c and Table 1. It can be found that the catalyst contains elements of carbon, silicon, calcium, sulfur and aluminum, originating from GAC. Moreover, the weight percentage of iron in FeO$_x$-GAC is 7.02%, which is close to the theoretical loading of 10%, suggesting that the iron oxides were successfully loaded on the activated carbon. The element mapping images in Fig. 1d confirming that Fe was uniformly distributed over the pores of the
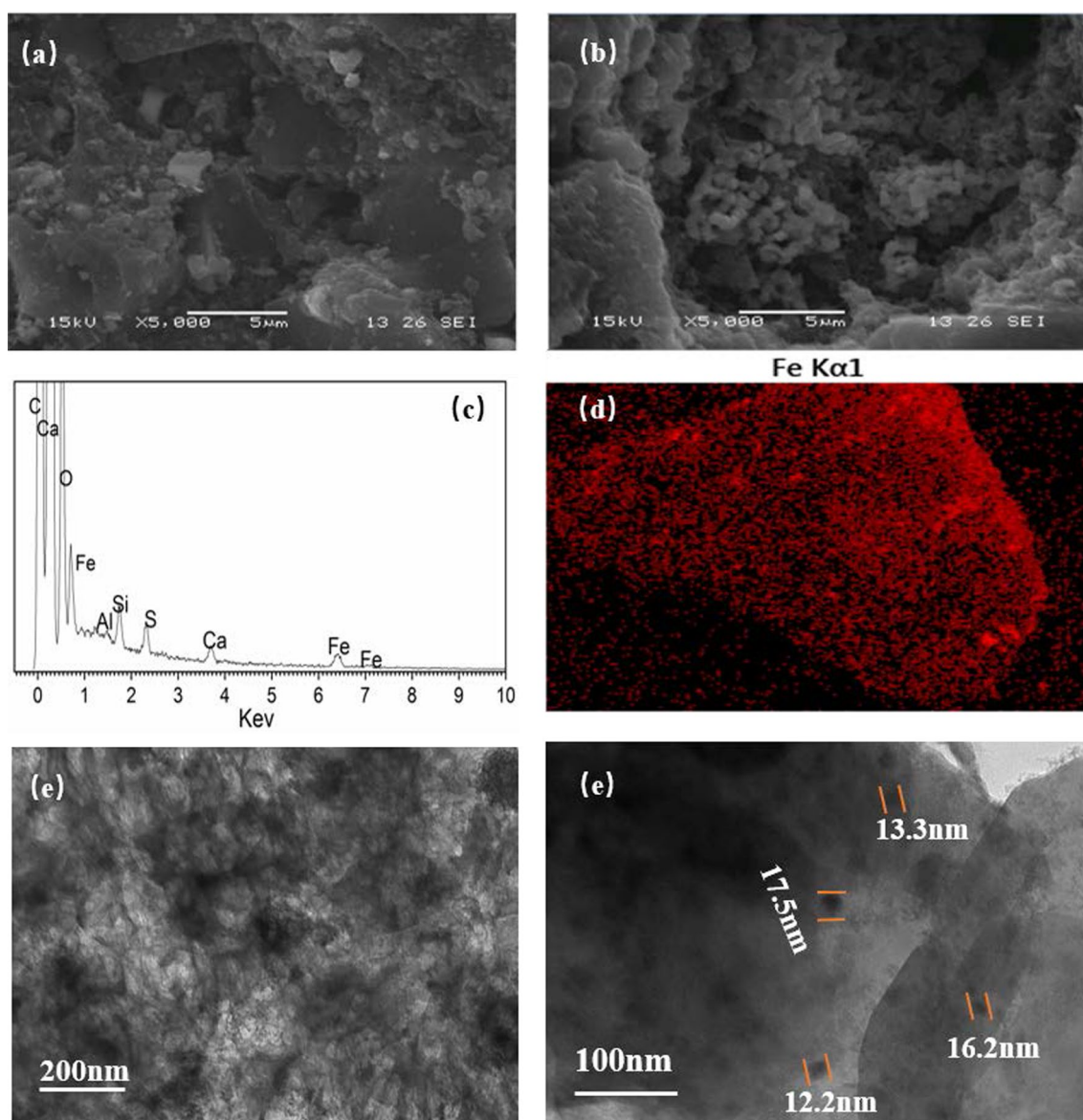

Fig.1 SEM image of GAC (**a**), FeO$_x$-GAC (**b**), EDS spectra of FeO$_x$-GAC (**c**), the element mapping images of FeO$_x$-GAC (**d**) and TEM image of FeO$_x$-GAC (**e**)

Table 1 Fe-GAC component content table

Element	Wt %	Atom %
C	78.39	87.22
O	11.94	9.97
Si	1.24	0.59
Ca	0.76	0.25
S	0.47	0.19
Fe	7.02	1.68
Al	0.18	0.09
Total	100.00	100.00

FeO_x-GAC. TEM was used to characterize the morphologies of the FeO_x-GAC, as shown in Fig. 1e. Dark zones were due to iron oxide whereas light parts indicated the presence of carbon, Qin et al. modified the parent activated carbon with urea and thiourea respectively, and obtained similar results with nitrogen doped activated carbon and nitrogen and sulfur co-doped activated carbon supported iron oxide (Fe/ACP, Fe/ACN and Fe/ACNS) catalysts [27]. It could be seen from the images that iron oxide was well spread on the carbon surface and only a very low number of iron oxide agglomerations. The size of the iron oxide agglomerations is 10-20 nm.

The changes of functional groups on the surface of FeO_x-GAC and GAC were investigated by infrared spectroscopy (Fig. 2). As can be seen from Fig. 2, there are four characteristic absorption peaks in the infrared spectrum of activated carbon: The absorption peak near 3433 cm^{-1} can be attributed to the typical -OH absorption, the peak near 2925 cm^{-1} is the stretching vibration of C-CH$_2$,Subrahmanyam et al. obtained the same result with us by FTIR spectra characterization of activated carbon fibers (ACF) [28], the peak near 1631 cm^{-1} is ascribed to the stretching vibration peak of C=C, and the peaks in the range
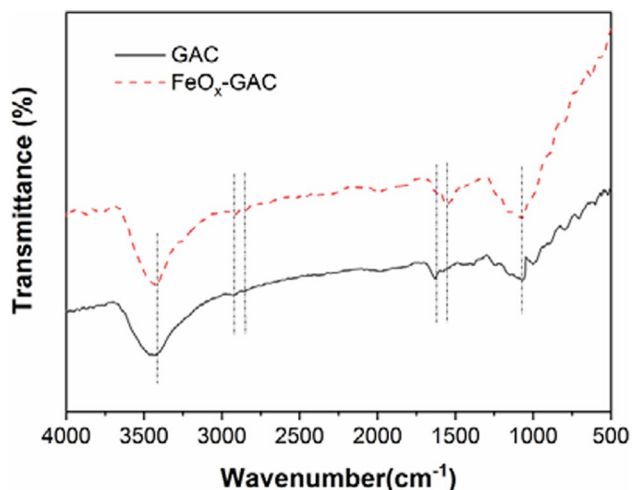
of 1000–1500 cm^{-1} correspond to the stretching vibration of C–OH and the bending vibration of -OH. Therefore, the surface of activated carbon is rich in oxygen-containing functional groups (i.e., -OH and -COOH), which can improve the hydrophilicity and stability of activated carbon in aqueous solution, similar results were obtained with the colloidal carbon nanospheres (CNS) synthesized by Song et al. [29]. The FeO_x-GAC also showed absorption peaks near 3433 cm^{-1}, 2925 cm^{-1}, 1631 cm^{-1}, and 1066 cm^{-1}, which are enhanced obviously in peak intensity comparing to those of GAC. Hence the amount of surface hydroxyl groups of FeO_x-GAC is increased, which further supports the potential of enhanced catalytic performance of the catalyst [30].

In the XRD spectra of GAC and FeO_x-GAC (Fig. 3), there are two distinctive diffraction peaks in both spectra of GAC and FeO_x-GAC (2θ = 25.6° and 43.3°), which correspond to the diffraction peaks of carbon crystals, these two distinctive diffraction peaks of carbon crystals are consistent with the XRD spectra of activated carbon prepared with oily sludge by Wang et al. [31, 32]. However, after loading iron component, the two characteristic peaks are weakened, indicating a decrease in the degree of crystallization of carbon. This may be attributed to the interaction between iron component and activated carbon during the loading of iron oxides, resulting in the misalignment and absence of carbon crystals [33]. The diffraction peaks associated with iron oxides were not observed on the catalyst surface, probably due to low content and the low crystallinity of iron oxides on the surface of activated carbon [34].

The results of XPS analysis of FeO_x-GAC are shown in Fig. 4. In the full spectrum scan of FeO_x-GAC (Fig. 4a), the main components of the catalyst are Fe, C and O. The Fe 2p peak in XPS spectrum clearly indicates that iron component has been successfully loaded on the activated carbon and is mainly present in the form of metal oxides.

Fig. 2 Infrared spectra of supported GAC and catalyst FeO_x-GAC
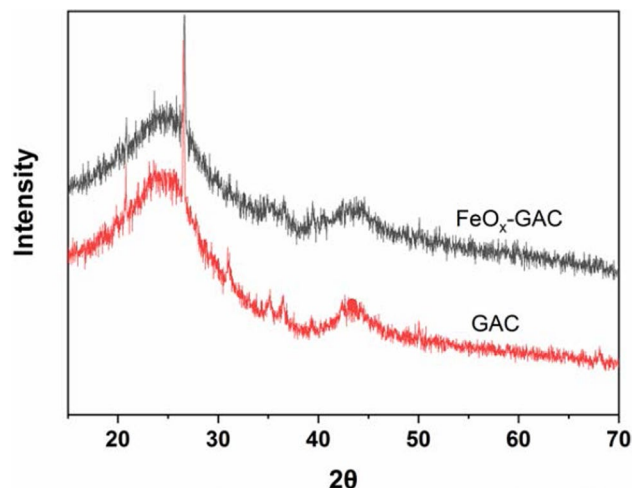
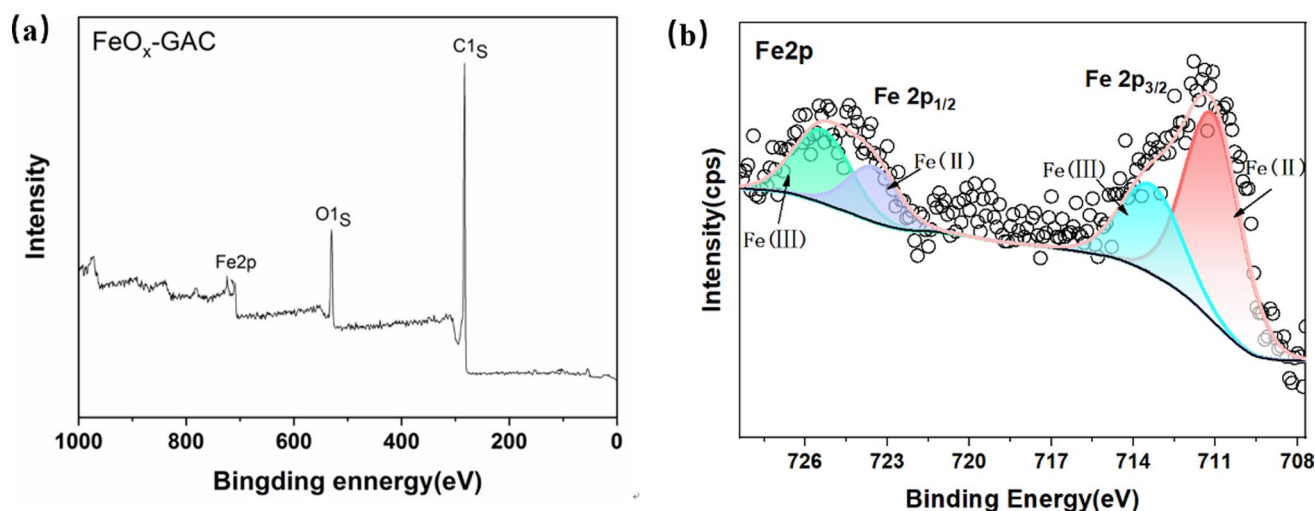**Fig. 3** XRD spectra of GAC and FeO_x-GAC

Fig. 4 **a** Full spectrum scan and **b** Fe 2p spectrum of XPS characterization for FeO$_x$-GAC.

As shown in Fig. 4b in the scan of Fe 2p, it can be clearly seen that there are two separated Fe 2p$_{3/2}$ and Fe 2p$_{1/2}$ electronic orbital states located at 710.0 ± 0.2 eV and 725.0 ± 0.2 eV, respectively. The Fe 2p orbital spectrum involves four characteristic peaks: Peaks at the binding energies of 711.1 eV and 723.5 eV can be attributed to the presence of Fe^{2+}, and peaks at 713.4 eV and 725.4 eV are attributed to the presence of Fe^{3+}. The results suggest that the oxidized iron loaded on activated carbon may be present in the form of divalent and trivalent ferric. Similar studies have been conducted by other researchers [35–37].

Degradation of metronidazole by catalytic ozonation

The degradation of metronidazole was evaluated in four processes: adsorption (GAC), ozonation (O$_3$), GAC catalytic ozonation (GAC/O$_3$) and FeO$_x$-GAC catalytic ozonation (FeO$_x$-GAC/O$_3$). In Fig. 5, metronidazole degradation in different systems can be observed and compared. The removal percentages of metronidazole through FeO$_x$-GAC/O$_3$ and GAC/O$_3$ were significantly higher than those through GAC adsorption and ozonation alone. Moreover, FeO$_x$-GAC/O$_3$ is more effective than GAC/O$_3$. The removal of metronidazole through GAC/O$_3$ was 38.62% at 6 min; while, the removal percentage of FeO$_x$-GAC/O$_3$ reached 51.26% that is 32.73% higher than that of GAC/O$_3$ process. After 9 min, the degradation of metronidazole in FeO$_x$-GAC/O$_3$ is 24.09% higher than that in GAC/O$_3$, and 70.73% higher than that of O$_3$ alone. Therefore, FeO$_x$-GAC/O$_3$ catalyst is of great catalytic activity and practical application.
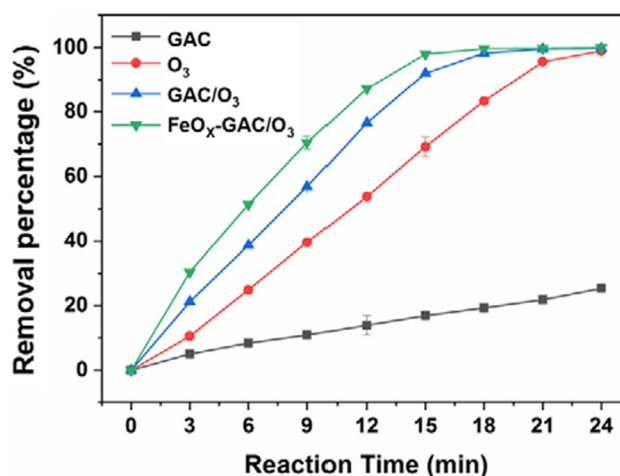

Fig. 5 Degradation of metronidazole in different reaction systems

Factors affected the metronidazole degradation in catalytic ozonation

The effect of ozone flow

Ozone flux is an important factor that control the catalytic ozonation [38]. In order to investigate the effect of ozone flow on the degradation of metronidazole in FeO$_x$-GAC/O$_3$ catalytic ozonation, the ozone flow was varied from 0.245 mg/min to 1.467 mg/min; while, other conditions were set constant, i.e., the FeO$_x$-GAC/O$_3$ dosage was 2 g/L, the applied ozone dosages was 24.45 mg/L, the initial concentration of metronidazole was 100 mg/L, and pH was adjust to neutral. The results are summarized in Fig. 6a. The removal rate of metronidazole gradually increased with the rate of ozone flow, and the
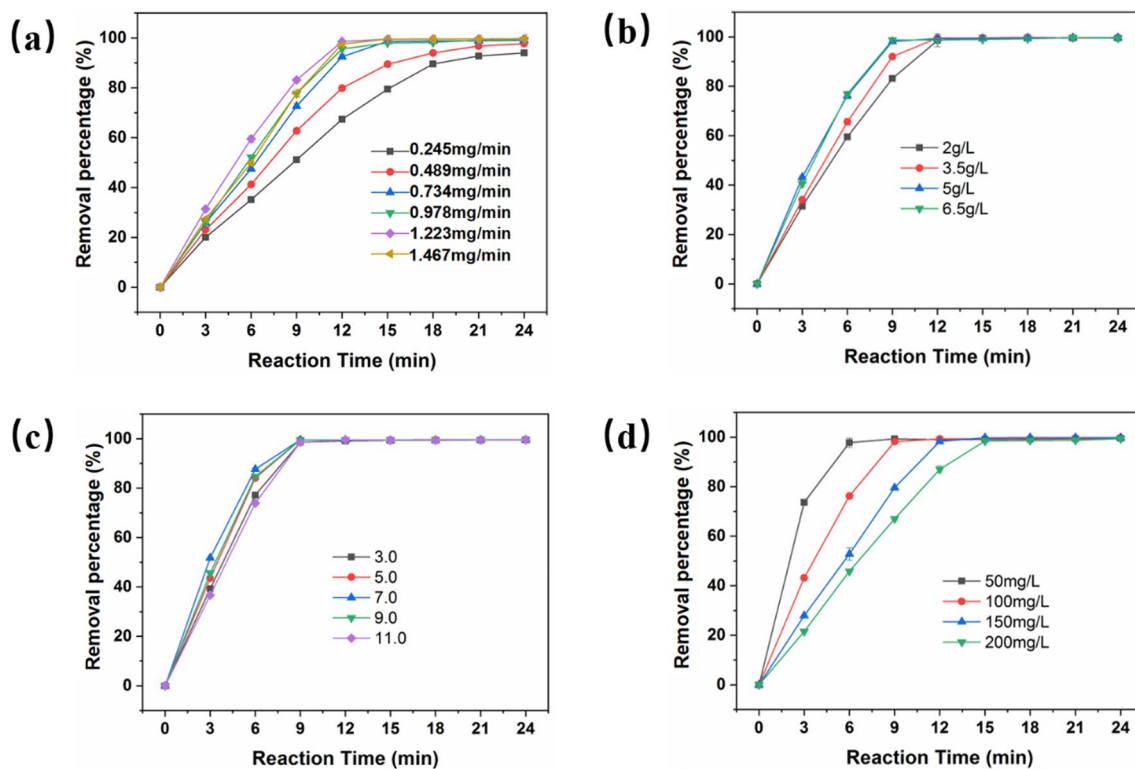
Fig. 6 Effects of different factors on metronidazole removal percentage (**a** O_3 flow, **b** catalyst dosage, **c** pH, and **d** initial concentration of metronidazole)

optimum removal efficiency was achieved at the ozone flow of 1.223 mg/min. However, when the amount of ozone increases to a higher level (e.g., 1.467 mg/min), the efficiency deteriorates. The free radicals produced in the aqueous solution could increase with the amount of ozone in the system. However, when too many radicals are existing in the system, the recombination of radicals or termination effect would happen [39]. Therefore, the optimal ozone flow is 1.223 mg/min.

The effect of catalyst dosage

The effect of catalyst dosage on the degradation of metronidazole is shown in Fig. 6b. The removal efficiency of metronidazole gradually improved with the catalyst dosage. However, when the catalyst dosage was increased to a level higher than 5 g/L (e.g., 6 g/L), the removal efficiency did not improve further. When the amount of catalyst is low, higher amount of catalyst can provide more active sites and accelerate the generation of free radicals facilitating the oxidation of metronidazole. Nevertheless, when there is too much catalyst, the produced redundant radicals would also have termination. Hence the optimum dosage of catalyst is determined to be 5 g/L.

The effect of pH The effect of pH on the efficiency of metronidazole degradation by catalytic ozonation is shown in Fi.6 (c). When the pH of metronidazole solution was acidic or alkaline, the removal of metronidazole was a little lower in efficiency. The highest removal efficiency was achieved when the pH was 7.0. At 6 min, the removal percentage in the system of pH 7.0 was about 12.82% and 18.92% higher than those of pH 3.0 and 11.0, respectively. Therefore, the pH should be adjusted to neutral in wastewater treatment.

Influence of initial concentration of metronidazole The effect of the initial concentration of metronidazole on the catalytic ozonation for the degradation of metronidazole is shown in Fig. 6d. The rate of catalytic ozonation decreases gradually with the concentration of metronidazole increasing. After 6 min, the removal percentage of 50 mg/L metronidazole could reach 97.78%, and the removal percentage of 200 mg/L metronidazole was only 66.99% although its reaction rate would be higher. Therefore, to ensure the treatment effectiveness, additional treatment time should be applied when high concentration of pollutant is in the system.

Mechanistic study of catalytic ozonation

UV–vis spectra analysis

The UV–vis scanning spectra of metronidazole degradation in catalytic ozonation process can be found in Fig. 7a. The characteristic absorption peak of metronidazole is located at 320 nm. The intensity of this absorption peak gradually decreased and finally disappeared during catalytic ozonation, which indicated that metronidazole was gradually degraded by catalytic ozonation [40]. Moreover, it can be seen that the intensity of peak around 220 nm gradually increased with time, indicating that the nitro and nitrogen-containing groups in the molecular structure of metronidazole could be attacked and generate nitrate [41] or other relevant byproducts [42].

Change of pH before and after the reaction of catalytic ozonation
In order to examine the pH change before and after the reaction of the catalytic ozonation, different initial pH was adjusted with acid or base for comparison test. The pH after the reaction was tested and the results are shown in Fig. 7b. In Fig. 7b, the yellow bar (pH) represents the pH before the reaction and the green bar (pH_{15}) represents the pH after 15 min of the reaction. Under acidic condi-

tions, the pH of the solution after the reaction remained unchanged and the solution remained acidic. When the initial pH was adjusted to 7, 9 or 11, the pH of the solution after the reaction decreased significantly. This indicates that during the ozone-catalyzed oxidation, metronidazole would be degraded into small molecules of acid and therefore the solution would be acidic. Besides, the presence of nitro group in the structure of metronidazole, the α-carbon of nitro group would be attacked by active oxidizing species in the catalytic ozonation and converts into nitrate [43]. Nitrate ions have been detected in the activated carbon catalyzed ozonation for the degradation of metronidazole by M. Sa´nchez-Polo et al. [43].

Free radical trapping experiment

Tert-Butanol (TBA) has the rate constants of 3×10^{-3} M^{-1} s^{-1} and 6×10^{8} M^{-1} s^{-1} for the reactions with ozone and ·OH, respectively. The rate constant for the reaction of TBA with ozone is much lower than that with ·OH, so the addition of tert-butanol to the system will quench the ·OH and prevent ·OH chain reaction [44, 45]. Therefore, TBA is generally chosen to capture ·OH in ozone reaction systems to explore the role of ·OH in catalytic ozonation. As shown in Fig. 7c, 0.1 mol/L TBA was added to the reaction system to explore

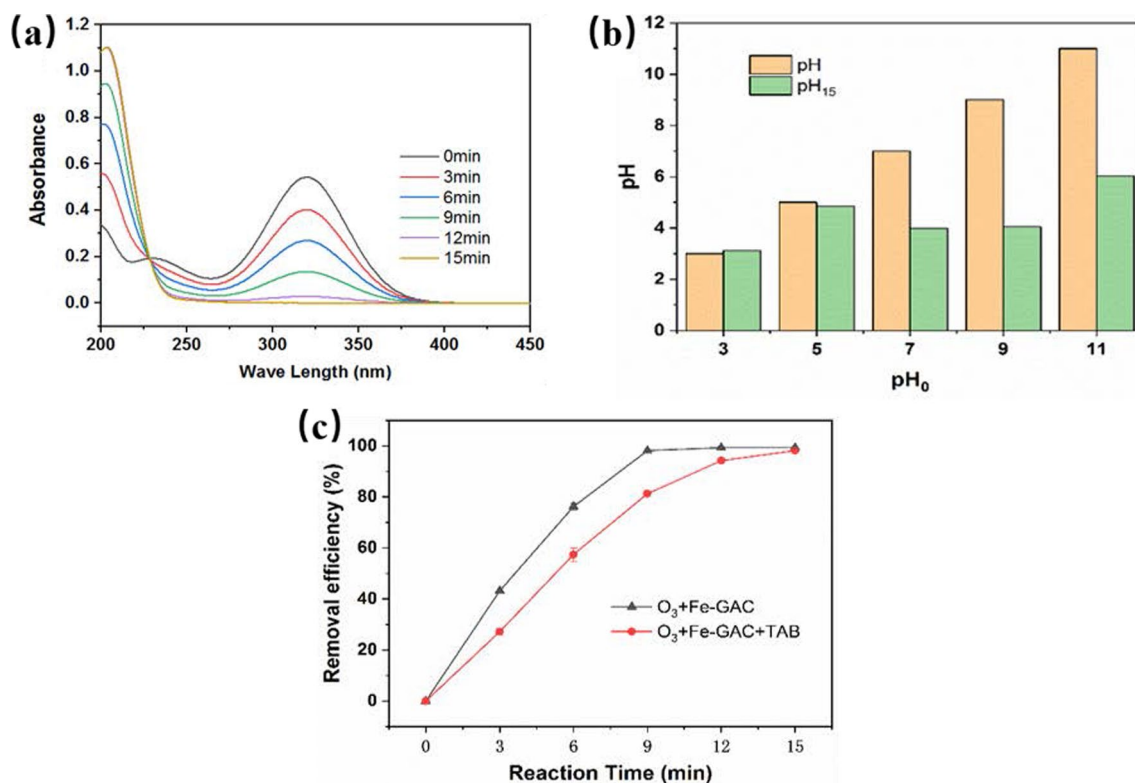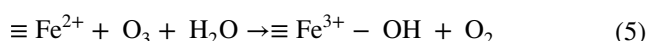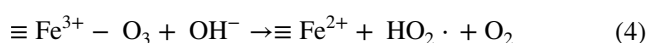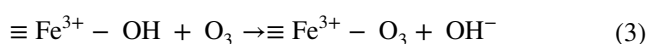**Fig. 7** **a** UV–Vis Spectral Scanning of metronidazole; **b** pH changes before and after the reaction; **c** the effect of TAB on the degradation of metronidazole.

the effect of ˙OH on the degradation of metronidazole in the experiment. It is obvious that there is a significant decrease in the rate of metronidazole removal. The degradation percentage of metronidazole in the FeO$_x$-GAC/O$_3$ system reached 98.19% after 9 min; while, the removal percentage only reached 81.29% after the addition of TBA, which reduced by 16.9%. This result indicates that the ˙OH radical is produced during catalytic ozonation, suggesting its role in the catalytic ozonation.

Combining free radical types and changes in element valence, the reaction equations are as follows [26, 46, 47]:

$$O_3 + HO^- \rightarrow O_2^{\cdot-} + HO_2\cdot \tag{1}$$

$$O_3 + HO_2^{\cdot} \Leftrightarrow 2O_2 + HO\cdot \tag{2}$$

$$\equiv Fe^{3+} - OH + O_3 \rightarrow \equiv Fe^{3+} - O_3 + OH^- \tag{3}$$

$$\equiv Fe^{3+} - O_3 + OH^- \rightarrow \equiv Fe^{2+} + HO_2\cdot + O_2 \tag{4}$$

$$\equiv Fe^{2+} + O_3 + H_2O \rightarrow \equiv Fe^{3+} - OH + O_2 \tag{5}$$

Conclusions

In this work, catalysts FeO$_x$-GAC for catalytic ozonation were prepared through impregnation–calcination approach and characterized by SEM, TEM, FTIR, XRD and XPS. The SEM images showed that the FeO$_x$-GAC had a porous structure, and further element mapping and TEM testing showed that Fe was uniformly distributed over the pores of the FeO$_x$-GAC. The degradation efficiency of metronidazole through FeO$_x$-GAC/O$_3$ and GAC/O$_3$ were compared. The results show that FeO$_x$-GAC/O$_3$ was more effective than GAC/O$_3$ in catalysis (24.09% more metronidazole was removed after 9 min). This is consistent with the conclusion of the amount of surface hydroxyl groups of FeO$_x$-GAC is increased by infrared spectroscopy. It indicates that the prepared FeO$_x$-GAC catalyst has high catalytic activity of ozone decomposition. The degradation of metronidazole through catalytic ozonation was affected by ozone dosing, catalyst dosing, pH and initial concentration of metronidazole, which were optimized in this work. When the initial metronidazole concentration is 100 mg/L, the optimal ozone dosing rate, catalyst dosing and pH should be 1.223 mg/min, 5 g/L and 7.0, respectively. It was also demonstrated that ·OH radicals were generated in the catalytic ozonation system. Based on the results of XPS, the main active sites of FeO$_x$-GAC for ozone activation were the Fe^{2+} and Fe^{3+} species on the surface of catalyst. This work provides fundamental data and

support for the practical application of FeO$_x$-GAC catalyst in catalytic ozonation.

Author contributions Na Wang:Conceptualization Methodology Formal analysis ResourcesChenxi Zhan:Writing - Review & Editing VisualizationJunzhuo Li:validationDan Liu:Writing - Original DraftJunjie Xiong:Data CurationGeshan Zhang:Writing - Review & EditingYin-an Ming:Supervision Conceptualization

Declarations

References

1. Carvalho IT, Santos L (2016) Antibiotics in the aquatic environments: a review of the European scenario. Environ Int 94:736–757
2. Bergeron S, Raj B, Nathaniel R et al (2017) Presence of of antibiotic resistance genes in raw source water of a drinking water treatment plant in a rural community of USA. Int Biodeterior Biodegradation 124:3–9
3. Mendez-Diaz JD, Prados-Joya G, Rivera-Utrilla J et al (2010) Kinetic study of the adsorption of nitroimidazole antibiotics on activated carbons in aqueous phase. J Colloid Interface Sci 345(2):481–490
4. Gomez MJ, Petrovic M, Fernandez-Alba AR et al (2006) Determination of pharmaceuticals of various therapeutic classes by solid-phase extraction and liquid chromatography-tandem mass spectrometry analysis in hospital effluent wastewaters. J Chromatogr A 1114(2):224–233
5. Saidi I, Soutrel I, Floner D et al (2014) Indirect electroreduction as pretreatment to enhance biodegradability of metronidazole. J Hazard Mater 278:172–179
6. Rosal R, Rodriguez A, Antonio P-M et al (2010) Occurrence of emerging pollutants in urban wastewater and their removal through biological treatment followed by ozonation. Water Res 44(2):578–588
7. De Wilt A, Van Gijn K, Verhoek T et al (2018) Enhanced pharmaceutical removal from water in a three step bio-ozone-bio process. Water Res 138:97–105
8. Jothinathan L, Hu J (2018) Kinetic evaluation of graphene oxide based heterogenous catalytic ozonation for the removal of ibuprofen. Water Res 134:63–73
9. Wang H, Huang Z, Jiang Z et al (2018) Trifunctional C@MnO catalyst for enhanced stable simultaneously catalytic removal of formaldehyde and ozone. ACS Catal 8(4):3164–3180
10. Guo Y, Wang H, Wang B et al (2018) Prediction of micropollutant abatement during homogeneous catalytic ozonation by a chemical kinetic model. Water Res 142:383–395
11. Qi F, Chu W, Xu B (2016) Comparison of phenacetin degradation in aqueous solutions by catalytic ozonation with CuFe$_2$O$_4$ and its precursor: Surface properties, intermediates and reaction mechanisms. Chem Eng J 284:28–36
12. Saeid S, Tolvanen P, Kumar N et al (2018) Advanced oxidation process for the removal of ibuprofen from aqueous solution: a non-catalytic and catalytic ozonation study in a semi-batch reactor. Appl Catal B-Environ 230:77–90
13. Zhang T, Li W, Croue J-P (2011) Catalytic ozonation of oxalate with a cerium supported palladium oxide: an efficient degradation

not relying on hydroxyl radical oxidation. Environ Sci Technol 45(21):9339–9346

14. Ghaffar A, Zhang L, Zhu X et al (2018) Porous PVdF/GO nanofibrous membranes for selective separation and recycling of charged organic dyes from water. Environ Sci Technol 52(7):4265–4274

15. Xiong Z, Lai B, Yang P (2018) Insight into a highly efficient electrolysis-ozone process for N, N-dimethylacetamide degradation: Quantitative analysis of the role of catalytic ozonation, fenton-like and peroxone reactions. Water Res 140:12–23

16. Biard P-F, Werghi B, Soutrel I et al (2017) Efficient catalytic ozonation by ruthenium nanoparticles supported on SiO2 or TiO2: Towards the use of a non-woven fiber paper as original support (vol 289, pg 374, 2016). Chem Eng J 315:639–639

17. Huo X, Liu J, Strathmann TJ (2018) Ruthenium catalysts for the reduction of N-nitrosamine water contaminants. Environ Sci Technol 52(7):4235–4243

18. Ndolomingo MJ, Meijboom R (2015) Kinetic analysis of catalytic oxidation of methylene blue over gamma-Al_2O_3 supported copper nanoparticles. Appl Catal Gen 506:33–43

19. Chen C, Yan X, Yoza BA et al (2018) Efficiencies and mechanisms of ZSM5 zeolites loaded with cerium, iron, or manganese oxides for catalytic ozonation of nitrobenzene in water. Sci Total Environ 612:1424–1432

20. Yan P, Ye Y, Wang M (2022) Catalytic ozonation of phenol by ZnFe(2)O(4)/ZnNCN: performance and mechanism. Environ Sci Pollut Res Int 29(58):88172–88181

21. Abdedayem A, Guiza M, Rivas Toledo FJ et al (2017) Nitrobenzene degradation in aqueous solution using ozone/cobalt supported activated carbon coupling process: a kinetic approach. Sep Purif Technol 184:308–318

22. Alvarez PM, Beltran FJ, Masa FJ et al (2009) A comparison between catalytic ozonation and activated carbon adsorption/ozone-regeneration processes for wastewater treatment. Appl Catal B-Environ 92(3–4):393–400

23. Bataineh H, Pestovsky O, Bakac A (2015) Iron(II) catalysis in oxidation of hydrocarbons with ozone in acetonitrile. ACS Catal 5(3):1629–1637

24. Borowska E, Bourgin M, Hollender J et al (2016) Oxidation of cetirizine, fexofenadine and hydrochlorothiazide during ozonation: Kinetics and formation of transformation products. Water Res 94:350–362

25. Bourgin M, Borowska E, Helbing J et al (2017) Effect of operational and water quality parameters on conventional ozonation and the advanced oxidation process O_3/H_2O_2: Kinetics of micropollutant abatement, transformation product and bromate formation in a surface water. Water Res 122:234–245

26. Yuan Y, Xing G, Garg S et al (2020) Mechanistic insights into the catalytic ozonation process using iron oxide-impregnated activated carbon. Water Res 177:115785

27. Qin H, Xiao R, Chen J (2018) Catalytic wet peroxide oxidation of benzoic acid over Fe/AC catalysts: effect of nitrogen and sulfur co-doped activated carbon. Sci Total Environ 626:1414–1420

28. Subrahmanyam C, Bulushev DA, Kiwi-Minsker L. Dynamic behaviour of activated carbon catalysts during ozone decomposition at room temperature. Appl Catal B Environ, 2005,61.

29. Song X, Gunawan P, Jiang R et al (2011) Surface activated carbon nanospheres for fast adsorption of silver ions from aqueous solutions. J Hazard Mater 194:162–168

30. Li W, Qiang Z, Zhang T et al (2012) Kinetics and mechanism of pyruvic acid degradation by ozone in the presence of PdO/CeO_2. Appl Catal B Environ 113:290–295

31. Wang J, Liu T-L, Huang Q-X et al (2017) Production and characterization of high quality activated carbon from oily sludge. Fuel Process Technol 162:13–19

32. Esohe Omoriyekomwan J, Tahmasebi A, Zhang J, et al. Synthesis of super-long carbon nanotubes from cellulosic biomass under microwave radiation. Nanomaterials (Basel), 2022,12(5).

33. Tang S, Yuan D, Zhang Q et al (2016) Fe-Mn bi-metallic oxides loaded on granular activated carbon to enhance dye removal by catalytic ozonation. Environ Sci Pollut Res 23(18):18800–18808

34. Xiong W, Chen N, Feng C et al (2019) Ozonation catalyzed by iron- and/or manganese-supported granular activated carbons for the treatment of phenol. Environ Sci Pollut Res 26(20):21022–21033

35. Zhu H, Ma W, Han H et al (2017) Catalytic ozonation of quinoline using nano-MgO: efficacy, pathways, mechanisms and its application to real biologically pretreated coal gasification wastewater. Chem Eng J 327:91–99

36. Singh A, Singh A, Singh S et al (2015) Synthesis, characterization and performance of zinc ferrite nanorods for room temperature sensing applications. J Alloy Compd 618:475–483

37. Lv A, Hu C, Nie Y et al (2010) Catalytic ozonation of toxic pollutants over magnetic cobalt and manganese co-doped gamma-Fe_2O_3. Appl Catal B-Environ 100(1–2):62–67

38. Lin F, Wang Z, Ma Q et al (2016) Catalytic deep oxidation of NO by ozone over MnO_x loaded spherical alumina catalyst. Appl Catal B 198:100–111

39. Xu R, Xiong J, Liu D et al (2022) Inverse micelle fabrication of ordered mesoporous manganese oxide and degradation of tetracycline hydrochloride. J Colloid Interface Sci 625:397–404

40. Khataee A, Kiransan M, Karaca S et al (2017) Photocatalytic ozonation of metronidazole by synthesized zinc oxide nanoparticles immobilized on montmorillonite. J Taiwan Inst Chem Eng 74:196–204

41. Perez T., Garcia-Segura S., El-Ghenymy A., et al. Solar photo-electro-Fenton degradation of the antibiotic metronidazole using a flow plant with Pt/air-diffusion cell and a CPC photoreactor. Abstracts of Papers of the American Chemical Society, 2015,250.

42. Yang J, Wang X, Zhu M et al (2014) Investigation of PAA/PVDF-NZVI hybrids for metronidazole removal: Synthesis, characterization, and reactivity characteristics. J Hazard Mater 264:269–277

43. Sanchez-Polo M, Rivera-Utrilla J, Prados-Joya G et al (2008) Removal of pharmaceutical compounds, nitroimidazoles, from waters by using the ozone/carbon system. Water Res 42(15):4163–4171

44. Nagarkatti MG (1991) Ozone in water treatment: application and engineering. J Environ Qual. https://doi.org/10.2134/jeq1991.00472425002000040040x

45. Potapenko EV, Andreev PY (2012) Catalytic oxidation of alkylbenzenes with ozone in acetic acid in the presence of strong acids. Pet Chem 52(2):113–118

46. Liu J, Peng C, Shi X (2022) Preparation, characterization, and applications of Fe-based catalysts in advanced oxidation processes for organics removal: a review. Environ Pollut 293:118565

47. Ikhlaq A, Brown DR, Kasprzyk-Hordern B (2013) Mechanisms of catalytic ozonation: An investigation into superoxide ion radical and hydrogen peroxide formation during catalytic ozonation on alumina and zeolites in water. Appl Catal B 129:437–449